Large Noncollinearity and Spin Reorientation in the Novel Mn_2RhSn Heusler Magnet

O. Meshcheriakova,[1,2] S. Chadov,[2] A. K. Nayak,[2] U. K. Rößler,[3] J. Kübler,[4] G. André,[5] A. A. Tsirlin,[2] J. Kiss,[2] S. Hausdorf,[2] A. Kalache,[2] W. Schnelle,[2] M. Nicklas,[2] and C. Felser[2]

[1]*Graduate School of Excellence "Materials Science in Mainz" Johannes Gutenberg—Universtität, 55099 Mainz, Germany*
[2]*Max-Planck-Institut für Chemische Physik fester Stoffe, Nöthnitzer Strasse 40, 01187 Dresden, Germany*
[3]*Leibniz-Institut für Festkörper-und Werkstoffforschung IFW, Helmholtz Strasse 20, 01171 Dresden, Germany*
[4]*Institut für Festkörperphysik, Technische Universität Darmstadt, 64289 Darmstadt, Germany*
[5]*Laboratoire Léon Brillouin, CEA-CNRS Saclay, 91191 Gif-sur-Yvette Cedex, France*

(Received 4 November 2013; revised manuscript received 13 May 2014; published 19 August 2014)

Noncollinear magnets provide essential ingredients for the next generation memory technology. It is a new prospect for the Heusler materials, already well known due to the diverse range of other fundamental characteristics. Here, we present a combined experimental and theoretical study of novel noncollinear tetragonal Mn_2RhSn Heusler material exhibiting unusually strong canting of its magnetic sublattices. It undergoes a spin-reorientation transition, induced by a temperature change and suppressed by an external magnetic field. Because of the presence of Dzyaloshinskii-Moriya exchange and magnetic anisotropy, Mn_2RhSn is suggested to be a promising candidate for realizing the Skyrmion state in the Heusler family.

DOI: 10.1103/PhysRevLett.113.087203 PACS numbers: 75.30.Kz, 75.10.Jm, 75.30.Et, 75.50.Gg

The art of controlling magnetic degrees of freedom has led to a broad range of applications that make up the rapidly developing field of spintronics. Up to now, most of the exploited compounds have been so-called collinear magnets, i.e., materials in which the magnetization is formed by local magnetic moments aligned parallel or antiparallel to one another. Yet, the possibility of influencing their mutual orientation opens new horizons for the field of spintronics. Noncollinear magnets can be widely applied in current-induced spin dynamics [1], magnetic tunnel junctions [2], molecular spintronics [3], spin-torque transfer by small switching currents [4], and anomalous exchange bias [5]. Impressive improvement of the critical current density by 5 orders of magnitude [6–8] is offered by noncollinear magnets driven into the Skyrmion phase [6–14]. While such exotic magnetic arrangements are sensitive to external conditions (magnetic field and temperature), an expansion of the related material base is important for their stabilization.

Flexible tuning of the magnetic properties can ultimately be realized in multicomponent systems of several magnetic sublattices with competing types of interactions such as magnetocrystalline anisotropy and dipole-dipole and Dzyaloshinskii-Moriya (DM) interactions [15,16]. Heusler compounds, of which there are over 1000 members, provide a rich variety of parameters for almost any material engineering task (e.g., half-metallic ferromagnetism [17,18], shape memory [19], exchange bias [20], topological insulators [21], spin-gapless semiconductivity [22], spin-resolved electron localization [23], and superconductivity [24]). Furthermore, the majority of Mn_2YZ (Y denotes a transition-metal atom and Z a main-group atom) systems are noncentrosymmetric; this together with the magnetocrystalline anisotropy induced by intrinsic tetragonal distortion makes such systems attractive for Skyrmion research.

First, we will discuss here the unusual ground-state magnetic canting observed in Mn_2RhSn together with the subsequent temperature-induced spin reorientation into the collinear ferrimagnetic mode. Further, we will give a detailed micromagnetic analysis which suggests this collinear regime to provide perfect conditions for the Skyrmion formation, in agreement with the earlier theoretical studies [9,25,26].

In a nonrelativistic case, the magnetic noncollinearity is a result of the competition between antiparallel and parallel exchange interactions (or between several types of antiparallel interactions). Such a situation is often encountered in Mn_2YZ compounds, but not all of them exhibit noncollinearity. In general, these materials crystallize in the noncentro-symmetric $I\bar{4}m2$ structure with two nonequivalent Wyckoff positions occupied by Mn atoms: Mn_I at $2b(0,\frac{1}{2},0)$ and Mn_{II} at $2d(0,\frac{1}{2},\frac{3}{4})$. Z and Y elements occupy the $2a(0,0,0)$ and $2c(0,\frac{1}{2},\frac{1}{4})$ positions, respectively [Fig. 1(a)]. The most significant exchange coupling between the nearest Mn_I and Mn_{II} atoms is characterized by a large exchange constant ($J_{Mn_I\text{-}Mn_{II}} \sim -20$ meV) (e.g., Ref. [27]) that leads to a typical collinear FiM (ferrimagnetic) state. Despite the fact that the in-plane interaction of Mn atoms can be rather complicated (e.g., the nearest in-plane neighbors couple parallel, the next-nearest couple antiparallel or parallel, and so on), these interactions are rather weak compared to $J_{Mn_I\text{-}Mn_{II}}$, which always aligns the Mn spin moments of the same plane parallel to one another [Fig. 1(b)]. For this reason, we initially do not consider the in-plane interactions but will expand the description in

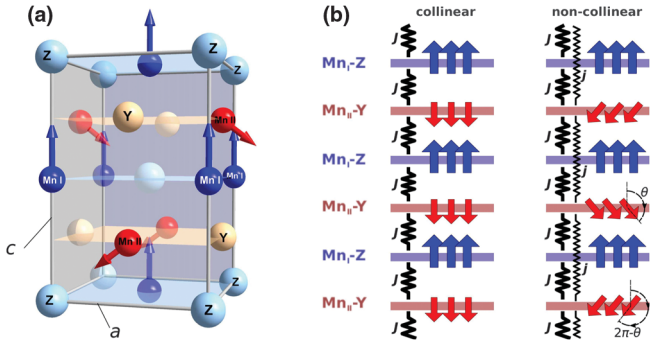

FIG. 1 (color). (a) Crystal and magnetic structures of Mn_2YZ Heusler compounds. Because of the magnetocrystalline anisotropy induced by the tetragonal distortion, the Mn_I magnetic moments are oriented along the c axis; the moments on Mn_{II} are canted in an alternating manner with respect to the c axis. (b) Schematic picture of the leading magnetic exchange interactions between different atomic layers in Mn_2YZ (atomic planes containing Z and Y elements are shown in blue and red, respectively). The arrows show the orientation of the spin moments on Mn, and the springs show the exchange interactions between different planes. Considering only the nearest antiparallel interactions J (between Mn_I-Z and Mn_{II}-Y planes) leaves the magnetic structure collinear; introducing the next-nearest antiparallel coupling j (between Mn_{II}-Y planes) leads to the alternating canting of Mn_{II} moments by θ and $2\pi - \theta$.

terms of the effective *interplane* exchange coupling J, which indicates the interaction of a certain Mn atom (i) with all other Mn atoms (i') in a different plane, i.e., $J = \sum_{i'} J_{ii'}$.

Since the collinear order being substantially determined by the nearest-plane J interaction becomes even more stable if the Y atom is magnetic (as, e.g., in case of Mn_2CoZ systems [27]), our further consideration concerns Mn_2YZ Heusler materials with the nonmagnetic heavy Y elements (such as Rh or Ir, since in the case of light elements, such as Ti or V, Mn atoms occupy equivalent $2c$ and $2d$ positions). In this case, the collinearity can be perturbed by the next important interaction j between the next-nearest planes, e.g., between pairs of Mn_{II}-Y planes, as shown in Fig. 1(b). This interaction is antiparallel due to its indirect origin realized through the main-group element Z (superexchange) [28]. Since j tends to rotate the moments of the nearest Mn_{II}-Y planes antiparallel to each other, it competes with the strong antiparallel exchange J and may then result in a nontrivial canting angle [$\theta \neq 0°, 180°$; see Fig. 1(b)]. The relevant θ-dependent part of the Heisenberg Hamiltonian will contain only antiparallel interactions:

$$H_\theta = -J\cos\theta - \frac{1}{2} j \cos 2(\pi - \theta), \qquad (1)$$

where the first term is the coupling of the nearest planes (Mn_I-Z with Mn_{II}-Y) and the second is that of the next-nearest (Mn_{II}-Y) planes. The factor $1/2$ accounts for the twice sparser entrance of the next-nearest-plane couplings. The extrema of H_θ are found from

$$\sin\theta\left(\frac{1}{2} + \frac{j}{J}\cos\theta\right) = 0, \qquad (2)$$

and $\theta_{1,2} = 180° \pm \arccos(J/2j)$ noncollinear solutions are given subject to the condition $j/J > \frac{1}{2}$, which means that the canting occurs only if the next-nearest antiparallel exchange j is sufficiently strong.

To justify the proposed magnetic order, we performed *ab initio* calculations (Supplemental Material [29], Sec. V) for Mn_2RhSn and another two similar Heusler systems Mn_2PtIn and Mn_2IrSn. For Mn_2RhSn, the plot of the total energy as a function of θ indeed exhibits two energy minima corresponding to the nontrivial canting angles $\theta_{1,2} = 180° \pm 55°$. Similar plots were obtained for another two compounds (Supplemental Material [29], Fig. S8). Calculated local moments, their orientations, total magnetization, and an experimentally measured one are summarized in Table I. These magnetic properties may be significantly affected by those kinds of disorder which are typical for Heusler systems. The details of this aspect are discussed in the Supplemental Material [29] (Sec. IV).

Powder neutron scattering data convincingly demonstrate the predicted ground-state noncollinearity (Fig. 2). At 1.8 K, the magnetic moments are $3.59\mu_B$ and $3.47\mu_B$ on Mn_I and Mn_{II}. The value obtained for the more localized Mn_I correlates with the calculated result (Table I), while the Mn_{II} moment is larger: it is defined less precisely as the scattering events on itinerant moments are more dispersed. The magnetic structure was found to be canted by about $\theta_{1,2} = (180 \pm 58.9)°$ within alternating Mn_{II}-Rh planes. It is important to note that such strong magnetic canting was never reported for the Heusler materials, in which it is typically of an order of a few degrees at most.

Being noncollinear in the ground state, the magnetic configuration evolves with changes to the temperature and external field. Observation of the (002) peak intensity for $T \leq 80$ K indicates the presence of in-plane magnetism [Fig. 2(b)]. As the temperature increases, the peak gradually decreases and subsequently vanishes for $T > 80$ K, suggesting that the in-plane magnetic component is suppressed [Fig. 2(b)]. This is attributed to the gradual spin

TABLE I. Computed atomic magnetic moments m, canting angles $\theta_{1,2}$, and total magnetization per formula unit $M = m_{Mn_I} + m_{Mn_{II}}\cos\theta + m_Y$, compared to the experimentally measured magnetization M_{exp}. Values of magnetic moments or magnetization are given in μ_B.

Mn_2YZ	m_{Mn_I}	$m_{Mn_{II}}$	$\theta_{1,2}$ (deg)	m_Y	M	M_{exp}
Mn_2RhSn	3.51	3.08	180 ± 55	0.14	1.9	1.97
Mn_2PtIn	3.38	3.30	180 ± 50	0.12	1.4	1.6
Mn_2IrSn	3.52	3.08	180 ± 44	0.09	1.4	1.5

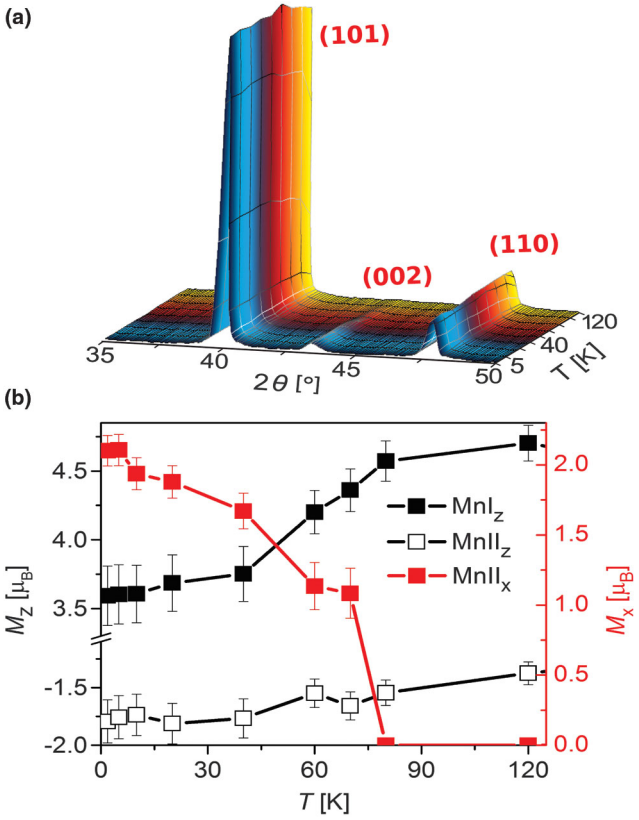

FIG. 2 (color). (a) Temperature-dependent neutron diffraction spectra. The (002) peak decays over 1.8–80 K. (b) Weakening of the in-plane magnetism (produced by the Mn_{II} x component) releases the z component of Mn_I, while the z component of Mn_{II} evolves rather insignificantly.

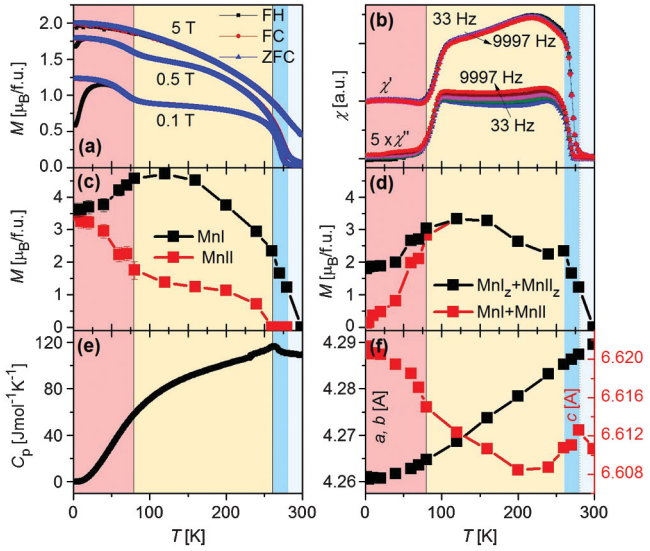

FIG. 3 (color). Evolution of the magnetic structure with the temperature. Canted (red regions), collinear ferrimagnetic (yellow regions), and disordered (blue regions) magnetic states of Mn_2RhSn. (a) Zero-field-cooled (ZFC), field-cooled (FC), and field-heated (FH) magnetization as a function of the temperature measured at induction fields of 0.1, 0.5, and 5 T. (b) Real (χ') and imaginary (χ'') ac-susceptibility components are frequency independent and show a pronounced step at the onset of the FiM phase. (c) The change in the canting angle occurs because of the simultaneous realignment of the Mn_{II} moment and a decrease in its absolute value. This, in turn, releases the previously suppressed Mn_I moment from $3.5\mu_B$ to $4.5\mu_B$. (d) The sum of the total and z components of the $Mn_{I(II)}$ moments follow the ac-susceptibility behavior. No in-plane component is present after 80 K. (e) A change in the slope of the heat capacity curve is observed in the vicinity of the spin reorientation. (f) Evolution of the lattice parameters with temperature: the change in the magnetism is echoed mainly by the c parameter, while a evolves monotonically.

reorientation of the Mn_{II} sublattice; the canting angle decreases until a collinear FiM order sets in at 80 K. Such behavior is strongly pronounced in the $M(T)$ curves measured in weak fields [0.1–0.5 T; see Fig. 3(a)] and suppressed in stronger fields (5 T). This is evidently an intrinsic effect, as the applied fields are larger than the coercive field ($H_c = 0.065$ T). It is not only the mutual orientation of the site-specific moments that changes but their absolute values that also change [Fig. 3(c)]. In the canted lowest-temperature state, the Mn_I moment is somewhat compensated by the equally strong Mn_{II}. As the temperature increases, the moments of Mn_{II} delocalize further and release the Mn_I to reach $4.5\mu_B$. This occurs gradually, and the slope of the zero-field heat capacity curve changes [Fig. 3(e)]; the spin-wave term is sufficiently weak in comparison to the electronic and phonon contributions such that no sharp anomaly is visible. However, the onset of the FiM phase is characterized by the explicit steplike increase in the ac-susceptibility signal [Fig. 3(b)]. Measured values of χ' and χ'' were found to be independent of the frequency, suggesting a high magnetic homogeneity. The evolution of the magnetism with temperature is echoed by the crystal structure [Fig. 3(f)]. Although the a parameter increases monotonically, the change in c parameter is nonlinear and corresponds to the ac-susceptibility behavior. The sudden rise in the vicinity of 280 K is an anomaly corresponding to T_C. The c parameter eventually decreases until a transition to the cubic phase occurs at about 570° C (Supplemental Material [29], Fig. S5).

By systematic coarse graining of the spin-lattice model, a micromagnetic continuum theory has been developed (Supplemental Material [29], Sec. VI). Considering only the leading Heisenberg-like exchange, the analysis shows that in tetragonal inverse Mn_2YZ Heusler alloys, the magnetic ordering displays coexisting magnetic modes with FiM of the two sublattices and an antiferromagnetic mode (AFM) on the Mn_{II} sublattice. These systems, thus, are close to a bicritical (or tetracritical) point in their magnetic phase diagram. In Mn_2RhSn, the thermodynamic potential favors a dominating collinear FiM order for $T > 80$ K. Below this temperature, the AFM sets in. By the crystal symmetry of Mn_2YZ, chiral inhomogeneous

DM couplings exist in spatial directions perpendicular to the crystal axis [25,26] that cause a spiral twist of these magnetic modes with long pitch. The micromagnetic model for the FiM state is exactly the Dzyaloshinskii model for a magnetic order in acentric tetragonal crystals from the $\bar{4}2m$ (D_{2d}) class [25,38]. Therefore, in the collinear FiM state, chiral Skyrmions and Skyrmion lattices exist in these magnets, as predicted in Refs. [9,25]. The micromagnetic model predicts a chiral twisting length $\Lambda \sim 130$ nm, which corresponds to the diameter of the FiM-state Skyrmions. These chiral Skyrmion states exist in the inverse Heusler alloys without the need of any additional effects not accounted for by the basic magnetic couplings, i.e., Heisenberg-like and DM exchange and leading anisotropies, and at arbitrary temperature. This is in contrast to chiral cubic helimagnets, which require fine-tuned additional effects for the existence of Skyrmionic states. Because the tetragonal lattice also induces a sizeable easy-axis magnetocrystalline anisotropy in Mn_2RhSn, as calculated by relativistic density functional theory, the magnetic phase diagram is not expected to display a field-driven condensed Skyrmion phase in this FiM state. The ratio of easy-axis anisotropy to DM coupling is large. Using the universal phase diagram of chiral magnets [9], Skyrmions do exist as nonlinear solitonic excitations of the collinear state in Mn_2RhSn. Therefore, this inverse Heusler alloy is an ideal system to realize reconfigurable nanomagnetic patterns composed of its two-dimensional free Skyrmions at elevated temperatures.

Coexistence of FiM and AFM orders in the canted state will be subject to different DM couplings. Thus, in the ground state, novel types of chirally twisted textures can exist in Mn_2YZ alloys. These chiral DM couplings favor different twisting lengths for the two modes and their interaction. Then, the magnetic order may become quasiperiodic and exceedingly complex, as recently described for the similar case of textures in biaxial nematic liquid crystals [39]. The presence of several DM terms and anisotropies affecting the coexisting magnetic modes promises a rich behavior of chiral textures in tetragonal inverse Heusler alloys Mn_2YZ. For example, closely below the onset of spin-reorientation temperature, the chiral Skyrmion of the FiM state is superimposed by a vortexlike AFM configuration on the Mn_{II} sublattice with a defect in the core of the soliton configuration. In the ground state, such configurations may become instable, depending on the stiffness of the AFM order. Up to now, such complex configurations have been analyzed only for the simpler case of chiral AFMs with a coexisting weak-FM mode [26].

As we have demonstrated theoretically and experimentally, the design of noncollinear magnets within the Heusler family of materials can be based on Mn_2YZ compositions, with Y and Z being a non- or weakly magnetic transition-metal element and a main-group element, respectively. The choice of the Mn_2YZ Heusler group allows us to control the canting angles by, e.g., combining the Y and Z elements or varying the Mn content. The use of heavy transition metals (e.g., as in the present case: Y = Pt, Rh, Ir and Z = Sn, In) amplifies the magnetically relevant relativistic effects that are already present in these systems, such as the DM interaction and magnetocrystalline anisotropy. Such multiple magnetic degrees of freedom together with the possibility of their manipulation provided by the family of Mn_2YZ Heusler materials are vital for the efficient engineering and stabilization of various magnetic orders. In particular, Mn_2RhSn is suggested to be a promising candidate for realizing the Skyrmion state in the Heusler family.

The authors thank A. Bogdanov, R. Stinshoff, and A. Beleanu for helpful discussions. The support of the European Commission under the 7th Framework Programme: Integrated Infrastructure Initiative for Neutron Scattering and Muon Spectroscopy: NMI3-II/FP7—Contract No. 283883, the Graduate School of Excellence "Materials Science in Mainz," the DFG Project FOR 1464 "ASPIMATT," and the European Research Council (ERC) for "Idea Heusler!" is gratefully acknowledged.

[1] P. Baláž, M. Gmitra, and J. Barnaś, Phys. Rev. B **80**, 174404 (2009).
[2] Y. Miura, K. Abe, and M. Shirai, Phys. Rev. B **83**, 214411 (2011).
[3] A. Soncini and L. F. Chibotaru, Phys. Rev. B **81**, 132403 (2010).
[4] N. L. Chung, M. B. A. Jalil, S. G. Tan, J. Guo, and S. B. Kumar, J. Appl. Phys. **104**, 084502 (2008).
[5] Y. F. Tian, J. F. Ding, W. N. Lin, Z. H. Chen, A. David, M. He, W. J. Hu, L. Chen, and T. Wu, Sci. Rep. **3**, 1094 (2013).
[6] F. Jonietz, S. Mühlbauer, C. Pfleiderer, A. Neubauer, W. Münzer, A. Bauer, T. Adams, R. Georgii, P. Böni, R. A. Duine, K. Everschor, M. Garst, and A. Rosch, Science **330**, 1648 (2010).
[7] X. Z. Yu, N. Kanazawa, W. Z. Zhang, T. Nagai, T. Hara, K. Kimoto, Y. Matsui, Y. Onose, and Y. Tokura, Nat. Commun. **3**, 988 (2012).
[8] T. Schulz, R. Ritz, A. Bauer, M. Halder, M. Wagner, C. Franz, C. Pfleiderer, K. Everschor, M. Garst, and A. Rosch, Nat. Phys. **8**, 301 (2012).
[9] A. N. Bogdanov and A. Hubert, J. Magn. Magn. Mater. **138**, 255 (1994).
[10] S. Mühlbauer, B. Binz, F. Jonietz, C. Pfleiderer, A. Rosch, A. Neubauer, R. Georgii, and P. Böni, Science **323**, 915 (2009).
[11] U. K. Rößler, A. N. Bogdanov, and C. Pfleiderer, Nature (London) **442**, 797 (2006).
[12] S. Seki, X. Z. Yu, S. Ishiwata, and Y. Tokura, Science **336**, 198 (2012).
[13] X. Yu, M. Mostovoy, Y. Tokunaga, W. Zhang, Y. M. Koji Kimoto, Y. Kaneko, N. Nagaosa, and Y. Tokura, Proc. Natl. Acad. Sci. U.S.A. **109**, 8856 (2012).

[14] P. Milde, D. Köhler, J. Seidel, L. M. Eng, A. Bauer, A. Chacon, J. Kindervater, S. Mühlbauer, C. Pfleiderer, S. Buhrandt, C. Schütte, and A. Rosch, Science **340**, 1076 (2013).
[15] I. Dzyaloshinsky, J. Phys. Chem. Solids **4**, 241 (1958).
[16] T. Moriya, Phys. Rev. **120**, 91 (1960).
[17] J. Kübler, A. R. Williams, and C. B. Sommers, Phys. Rev. B **28**, 1745 (1983).
[18] R. A. de Groot, F. M. Mueller, P. G. van Engen, and K. H. J. Buschow, Phys. Rev. Lett. **50**, 2024 (1983).
[19] R. Kainuma, Y. Imano, W. Ito, Y. Sutou, H. Morito, S. Okamoto, O. Kitakami, K. Oikawa, A. Fujita, T. Kanomata, and K. Ishida, Nature (London) **439**, 957 (2006).
[20] A. K. Nayak, M. Nicklas, S. Chadov, C. Shekhar, Y. Skourski, J. Winterlik, and C. Felser, Phys. Rev. Lett. **110**, 127204 (2013).
[21] S. Chadov, X.-L. Qi, J. Kübler, G. H. Fecher, C. Felser, and S.-C. Zhang, Nat. Mater. **9**, 541 (2010).
[22] S. Ouardi, G. H. Fecher, C. Felser, and J. Kübler, Phys. Rev. Lett. **110**, 100401 (2013).
[23] S. Chadov, J. Kiss, and C. Felser, Adv. Funct. Mater. **23**, 832 (2013).
[24] T. Klimczuk, C. H. Wang, K. Gofryk, F. Ronning, J. Winterlik, G. H. Fecher, J.-C. Griveau, E. Colineau, C. Felser, J. D. Thompson, D. J. Safarik, and R. J. Cava, Phys. Rev. B **85**, 174505 (2012).
[25] A. N. Bogdanov and D. A. Yablonskii, Sov. Phys. JETP **68**, 101 (1989).
[26] A. N. Bogdanov, U. K. Rössler, M. Wolf, and K.-H. Müller, Phys. Rev. B **66**, 214410 (2002).
[27] M. Meinert, J.-M. Schmalhorst, and G. Reiss, J. Phys. Condens. Matter **23**, 116005 (2011).
[28] H.-B. Luo, Q.-M. Hu, C.-M. Li, B. Johansson, L. Vitos, and R. Yang, J. Phys. Condens. Matter **25**, 156003 (2013).
[29] See Supplemental Material at http://link.aps.org/supplemental/10.1103/PhysRevLett.113.087203, which includes Refs. [30–37], for experimental details/results on structural/chemical/magnetic characterization, details/results of the *ab initio* calculations, construction and analysis of the micromagnetic continuum theory.
[30] J. Rodríguez-Carvajal, computer code FULLPROF, LLB, 2004.
[31] V. Alijani, O. Meshcheriakova, J. Winterlik, G. Kreiner, G. H. Fecher, and C. Felser, J. Appl. Phys. **113**, 063904 (2013).
[32] A. K. Nayak, C. Shekhar, J. Winterlik, A. Gupta, and C. Felser, Appl. Phys. Lett. **100**, 152404 (2012).
[33] J. Kiss, S. Chadov, G. H. Fecher, and C. Felser, Phys. Rev. B **87**, 224403 (2013).
[34] H. Ebert, D. Ködderitzsch, and J. Minár, Rep. Prog. Phys. **74**, 096501 (2011).
[35] S. H. Vosko, L. Wilk, and M. Nusair, Can. J. Phys. **58**, 1200 (1980).
[36] A. I. Liechtenstein, M. I. Katsnelson, V. P. Antropov, and V. A. Gubanov, J. Magn. Magn. Mater. **67**, 65 (1987).
[37] H. Ebert and S. Mankovsky, Phys. Rev. B **79**, 045209 (2009).
[38] I. E. Dzyaloshinskii, Sov. Phys. JETP **19**, 960 (1964).
[39] V. L. Golo, E. I. Kats, A. A. Sevenyuk, and D. O. Sinitsyn, Phys. Rev. E **88**, 042504 (2013).